

²⁴A. Kawabata, J. Phys. Soc. Jap. **29**, 902 (1970).

²⁵R. Dupree and M. A. Smithard, J. Phys. C **5**, 408 (1972).

²⁶M. J. Rice and J. Bernasconi, Phys. Rev. Lett. **29**, 113 (1972).

²⁷To our knowledge, of the two-spacing approximate

distributions only the orthogonal case has been calculated analytically; the result was given by Porter. See his book listed in Ref. 8.

²⁸P. B. Kahn, Nucl. Phys. **41**, 159 (1963).

PHYSICAL REVIEW B

VOLUME 7, NUMBER 8

15 APRIL 1973

Determination of the Surface Geometry for the Aluminum (110) and (111) Surfaces by Comparison of Low-Energy-Electron-Diffraction Calculations with Experiment

M. R. Martin and G. A. Somorjai

Inorganic Materials Research Division, Lawrence Berkeley Laboratory, and Department of Chemistry, University of California, Berkeley, California 94720

(Received 20 September 1972; revised manuscript received 6 November 1972)

Low-energy-electron-diffraction calculations have been extended to the (110) and (111) surfaces of aluminum in order to determine the spacing between the surface and bulk layers of the crystal. The Al(110) surface is found to be contracted by 10% to 15% from the bulk interlayer spacing, and the Al(111) surface is found to deviate from the bulk spacing by less than 5%. This amounts to a determination of the surface-layer position to within 0.1 Å. Results of calculations on all experimentally measured beams for these surfaces are compared with the experimental results for several assumed interlayer spacings. These comparisons are made with respect to qualitative peak shapes, peak positions, and relative peak amplitudes of the specular and all measured nonspecular beams from each surface. In order to achieve this agreement, it has been necessary to include the four outermost crystal layers and to describe the ion-core potential with five phase shifts in the 40–150-eV energy range.

I. INTRODUCTION

Encouraging progress has been made recently on the problem of crystal-surface-structure analysis by low-energy-electron diffraction (LEED). Several theoretical approaches to the multiple-scattering problem have led to the assembly of a variety of computer programs whose results have appeared recently in the literature. Multiple scattering has been taken into account by calculations based on a band-structure approach,¹⁻³ a *t*-matrix approach,⁴⁻⁶ and the layer Korringa-Kohn-Rostoker (KKR) method.^{7,8} In addition, two perturbation methods have been proposed to reduce the computer-time requirements of the more exact methods.⁹⁻¹¹

In this paper we report on LEED calculations performed on several beams of the aluminum (110) and (111) surfaces. In Sec. II we describe the multiple-scattering method employed to construct the computer program. In Sec. III we discuss the parameters used throughout the calculations, and in Secs. IV and V we present the results of the aluminum (110) and (111) calculations, respectively, and compare them with experiment.

These calculations indicate that the position of the surface layer with respect to the bulk can be determined to within ~5% of the bulk interlayer spacing. The Al (110) surface layer is found to be located between 1.285 and 1.214 Å from the next-underlying layer which represents a contraction of

10–15% from the bulk interlayer spacing. The Al (111) surface-layer spacing is found to be equal to the bulk interplane spacing to within ~5%. In each case the surface-layer spacing is determined to within 0.1 Å.

II. DESCRIPTION OF CALCULATION

The computer program we have developed is based on the *t*-matrix approach to the multiple-scattering problem as formulated by Beeby,⁴ and extended by Duke and Tucker⁵ to include inelastic damping of the electron beam. The reader is referred to a paper by Laramore and Duke¹² in which the formalism that we employ in our calculation is set forth. Finite-temperature effects are accounted for in the Debye approximation, and the bulk lattice and surface layer can be assigned different Debye temperatures.

The scattering amplitude from a subplane λ , parallel to the surface, is proportional to a quantity $T_\lambda(\vec{k}_f, \vec{k}_i; E)$ [see Ref. 12, Eq. (3)], which is the *t*-matrix element for scattering from an incident plane wave whose wave vector is \vec{k}_i into an outgoing wave \vec{k}_f , at constant energy E . This quantity is expanded in an angular-momentum representation and one is concerned with evaluating a square matrix of dimension $(l+1)^2 \times (l+1)^2$, $T_\lambda^{LL'}$, where l is the angular-momentum quantum number corresponding to the highest-order phase shift $[\delta_l(E)]$ used to characterize the ion-core potential.

The evaluation of this matrix can be accomplished

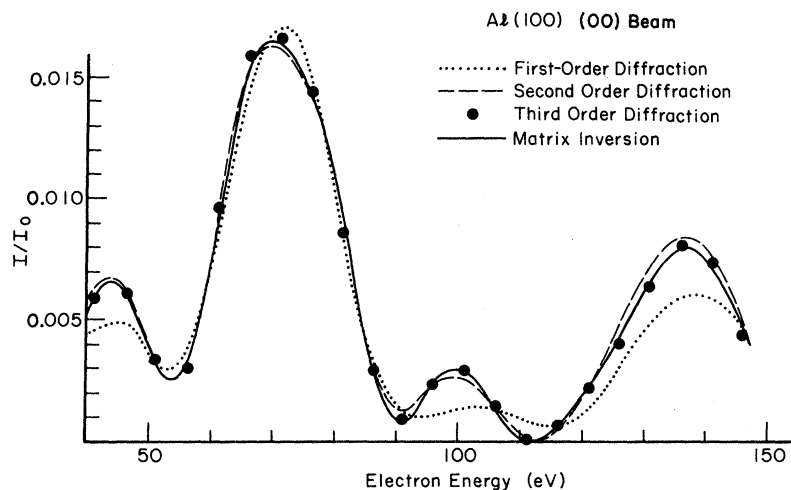


FIG. 1. Intensity curves for the (00) beam of the aluminum (100) surface as a function of incident-electron energy calculated with three layers and five phase shifts. The single-scattering (kinematic) intensity curve is compared to curves obtained from a dynamic calculation with double diffraction, triple diffraction, and the "matrix-inversion" result.

by means of a matrix-inversion technique,¹³ or by use of a perturbation series expansion. Perturbation calculations have been reported in the literature which truncate the expansion at second^{6,9} and third order.¹⁰ The method employed in this paper is to perform a perturbation expansion of arbitrary order which should approach the true matrix-inversion result if enough terms are included and provided the ion-core scattering matrix $t_\lambda(\vec{k}_f, \vec{k}_i; E)$ is not too large.¹⁴ In Fig. 1 we present the results for such calculations on the (100) surface of aluminum. It is seen that for the (00) beam of this surface, the convergence is rapid and that no new features emerge beyond the second order of the expansion.

The iterative method was compared to the true matrix-inversion method in the evaluation of the quantity $\tau_\lambda(\vec{k}_f, \vec{k}_i; E)$, which is the t matrix for the scattering of an incident wave \vec{k}_i into a final wave \vec{k}_f from subplane λ , in the absence of any other subplanes. The iterative method is found to be up to 20% faster in computer-time requirements and generally converges in fewer than ten iterations. The subplane and interplane propagators $G_{L_1 L_2}^{sp}(\vec{k}_i)$ and $G_{L_1 L_2}^{\lambda \lambda_1}(\vec{k}_i)$ were calculated using Eqs. (46) and (50) of Ref. 12.

III. PARAMETERS USED IN CALCULATION

The scattering potential at a lattice site is specified by a number of precalculated energy-dependent phase shifts $\delta_i(E)$. These phase shifts may be obtained at present from self-consistent augmented-plane-wave (APW) potentials¹⁵ or by the *ab initio* method of Pendry.¹⁶ Apparently, the description of the scattering process by these two methods is of sufficient accuracy to yield qualitatively correct theoretical beam-intensity-versus-incident-electron-energy (I - eV) curves.

The first numerical results obtained by Duke and

Tucker^{5,6} were based on an s -wave approximation to the scattering amplitudes. Since that time, calculations for aluminum have appeared utilizing from three to eight phase shifts.^{7,9,10,17,18} In Fig. 2 we plot the I - eV curve for the (100) face (00) beam of aluminum. The plots are for normal in-

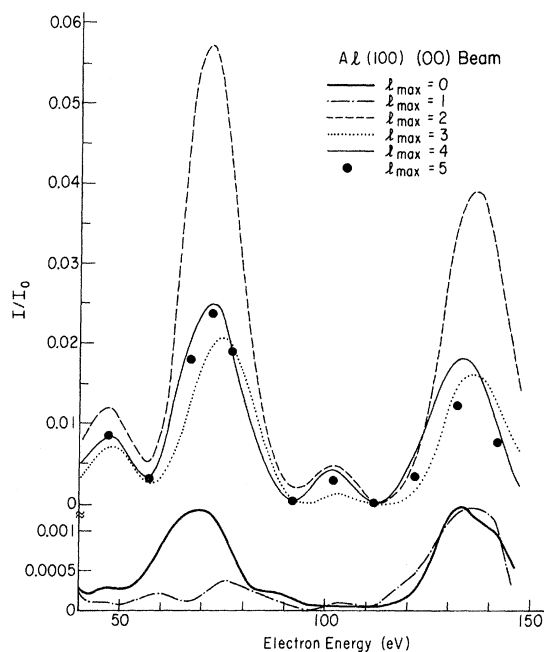


FIG. 2. Calculated (00) beam intensity vs incident electron energy for a normally incident beam on the aluminum (100) surface including the five outermost layers. The lower two curves are computed using Pendry's ion-core potential with one and two phase shifts. The intensity scale of the lower curves is ten times that of the upper curves. The labeled l_{max} values refer to the largest angular-momentum quantum number whose phase shift $\delta_{l_{max}}(E)$ appears in the summation.

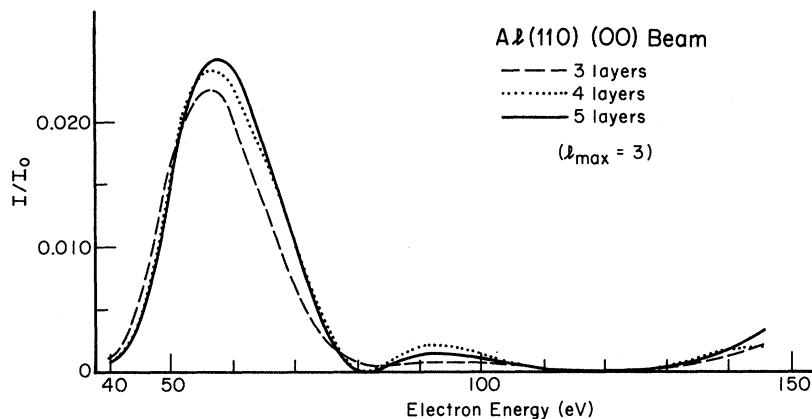


FIG. 3. Comparison of I -vs- eV curves computed using four phase shifts and three, four, and five crystal layers parallel to the aluminum (110) surface.

cidence of the electron beam, with the sample temperature at 298 K [$\Theta_D(\text{surf}) = \Theta_D(\text{bulk}) = 426$ K]. Five surface layers have been included in the calculation. Throughout this paper we employ the ion-core potential obtained from a computer program supplied by Pendry.¹⁹ The first four of these phase shifts agree with those reported by Tong and Rhodin⁹ and will thus not be reproduced here.

Although no experimental results exist for normally incident (00) beams, the curves thus obtained using five or six phase shifts bear a close qualitative resemblance to experimental results whose incident beam impinges at 6° from the normal. From Fig. 2 it is apparent that the I -vs- eV curves calculated using only the first two phase shifts are poor approximations to the observed intensity patterns. Furthermore, the intensity scale of the lower curves compared to that of the upper curves, in which three or more phase shifts are included, shows that an almost insignificant portion of the total scattering power arises from the first two partial waves. The upper set of curves in Fig. 2 demonstrates a remarkable qualitative similarity between all curves which include more than two phase shifts. Tong and Rhodin have pointed out the dominance of d -wave scattering for energies in excess of 24 eV.⁹ Equally striking, however, is the sharp decrease in scattered intensity upon adding the $l=3$ phase shift to the calculation. Peak positions are altered by up to 2 eV as each additional phase shift is included. The two most intense peaks (corresponding closely to the locations of single scattering or kinematic peaks) appear to be most sensitive to this variation, whereas the two smaller multiple-scattering peaks are more stable with regard to peak location. Marcus *et al.*²⁰ have shown that for the (100) surface of aluminum the inclusion of four layers parallel to the surface yields substantial agreement to a treatment including the entire semi-infinite solid. In Fig. 3 we confirm this result for the (110) surface of

aluminum by plotting intensity curves in which three, four, and five layers are included. We use four layers in all subsequent calculations.

In the present work we have concentrated on calculating the LEED intensity curves for all experimentally measured beams²¹ of the aluminum (110) and (111) surfaces. In Fig. 4 we show the beam geometry used in these calculations. We in-

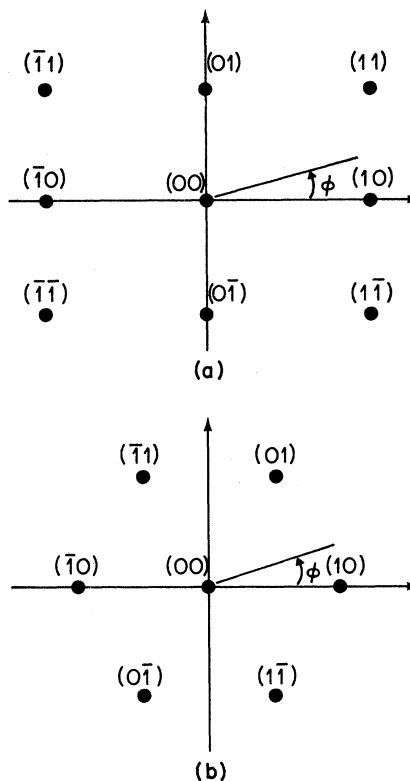


FIG. 4. LEED spot positions for (a) the (110) surface and (b) the (111) surface of aluminum. The spot labels and the azimuthal angles ϕ are defined to be identical to those of Jona (Ref. 21).

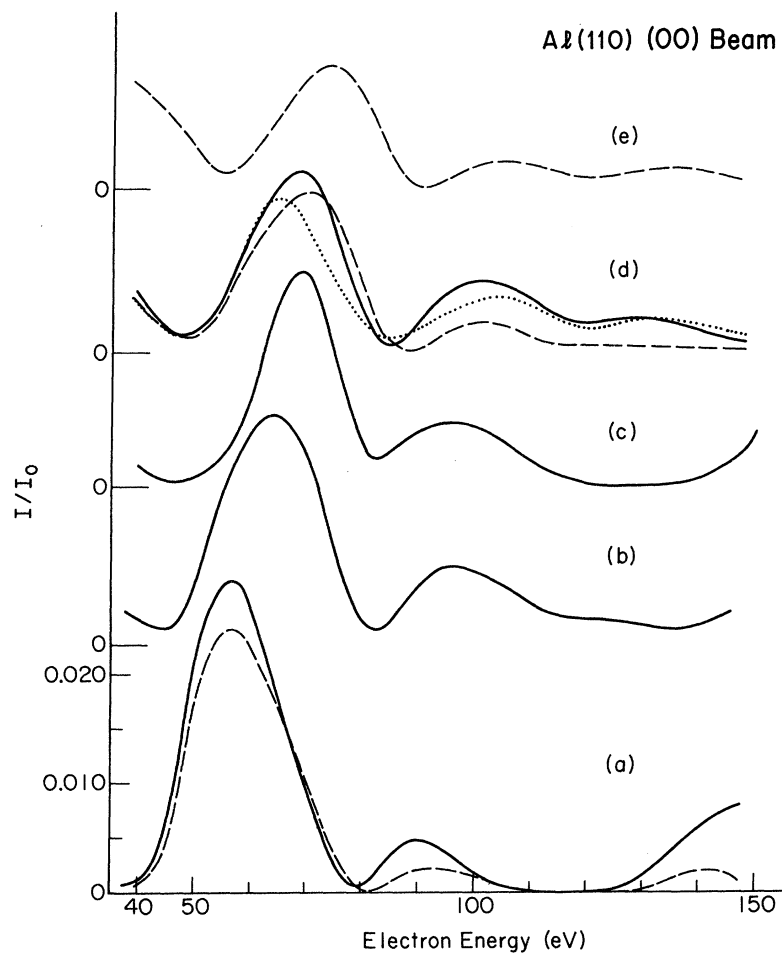


FIG. 5. Experimental I -vs- eV curve (c) is compared to calculated curves for the (00) beam of the aluminum (110) surface. The solid curves [(a), (b), (d)] and the dotted curve (d) utilize five phase shifts and four layers in the computation. The dashed curves utilize four phase shifts and four layers. Curve (a) is obtained from an undistorted surface (i.e., interlayer spacing equal to the bulk value 1.43 Å). In curve (b) the outer layer is contracted by 15% to 1.214 Å, and in curve (e) it is contracted by 20% from the bulk value to 1.142 Å. Curve (d) is computed for incident beam angles $\theta = 5^\circ$ and $\phi = 90^\circ$, which are the same angles as measured for the experimental curve (c). The remaining curves are calculated at normal incidence. The theoretical curves are all shifted by 3.65 eV to account for the metallic work function.

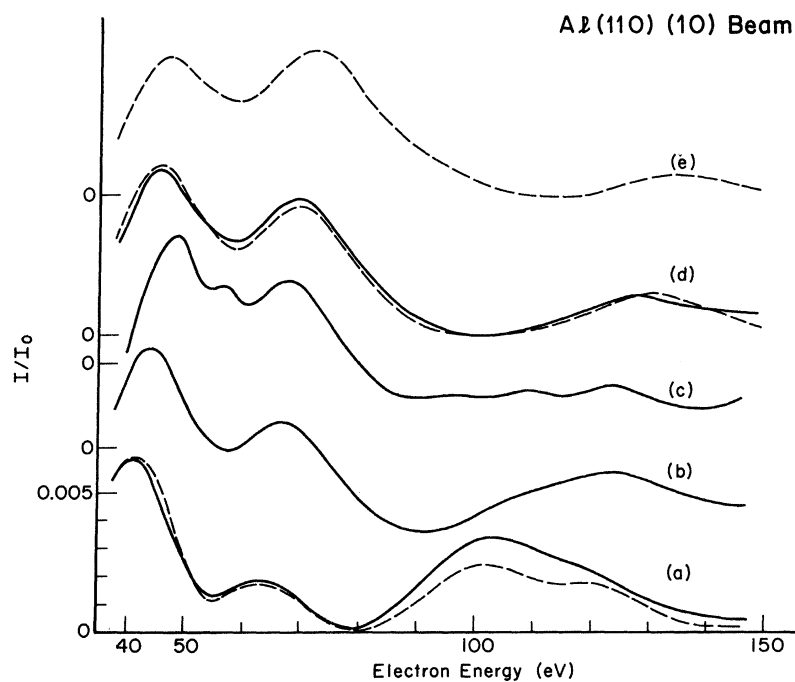


FIG. 6. Experimental I -vs- eV curve (c) is compared to calculated curves for the (10) beam of the aluminum (110) surface. The descriptions of curves (a)–(e) are given in the caption to Fig. 5. All curves are computed or measured at normal incidence.

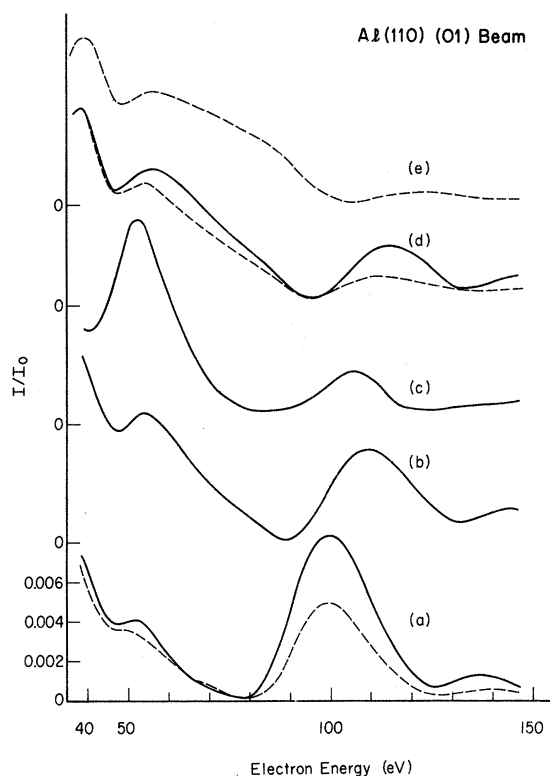


FIG. 7. Experimental I -vs- eV curve (c) is compared to calculated curves for the (01) beam of the aluminum (110) surface. The descriptions of curves (a)–(e) are given in the caption to Fig. 5. All curves are computed or measured at normal incidence.

clude only results obtained for incoming beams at or near normal incidence. From an experimental point of view, normal incidence can be determined to a greater degree of accuracy than other angles can be measured. From a theoretical point of view, one would expect the beams incident at large angles to the normal to be more sensitive to details of the surface (i.e., directional properties in the electron gas, dipole-layer effects, etc.) than beams at or near normal incidence. Furthermore, we have restricted our incident-energy range to energies in excess of 40 eV. Small stray fields in the vicinity of the sample will deflect an incident beam of low energy more than they will a higher-energy beam. Also, several models for the electron self-energy within the metal have been proposed. These models, which include the free-electron-gas calculation by Lundqvist²² and the optical-model potential⁷ are in substantial agreement over a wide energy range for $E > 40$ eV. In the 20-eV region, the real and imaginary parts of the self-energy predicted by the Lundqvist model differ considerably from the constant values assumed in the optical model. We use 150 eV as the upper limit of our calculations because of the greater number of phase shifts necessary to adequately characterize the ion-core potential at higher energies.

IV. ALUMINUM (110)

Of the three low-order surfaces of aluminum, the (110) face has proved to be the most elusive in

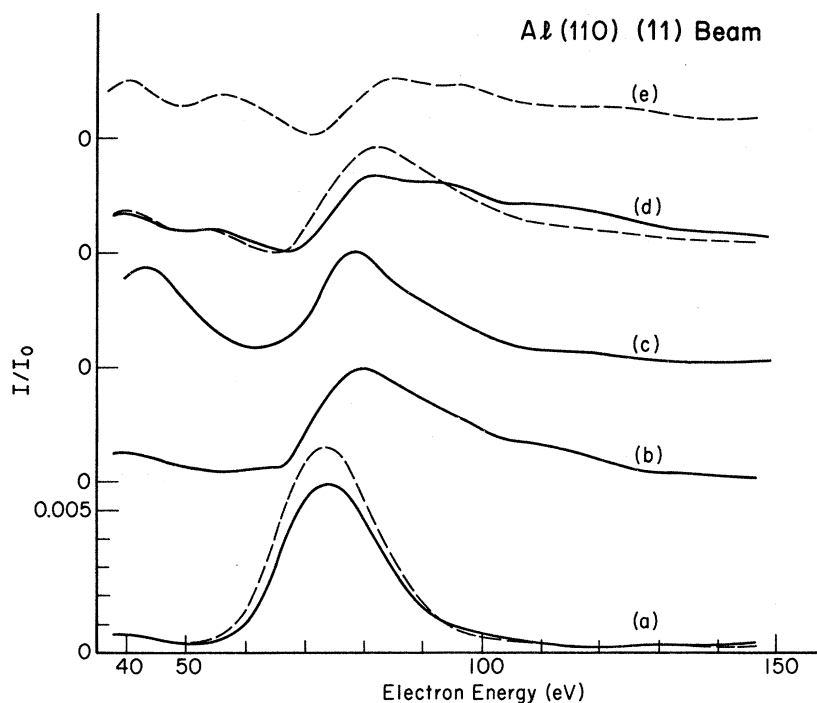


FIG. 8. Experimental I -vs- eV curve (c) is compared to calculated curves for the (11) beam of the aluminum (110) surface. The descriptions of curves (a)–(e) are given in the caption to Fig. 5. All curves are computed or measured at normal incidence.

achieving theoretical agreement with the experimental results. Laramore and Duke¹⁷ have recently investigated the (100), (110), and (111) surfaces using a maximum of three phase shifts and treating the surface region as a simply truncated bulk crystal. They suggest that the discrepancies in the case of the (110) surface could be due to a contraction in the spacing between the two outermost layers of the order of 10%. Laramore, Houston, and Park²³ have taken a different approach and attempt to account for the disagreement between theory and experiment by proposing that the aluminum (110) surface is not a simple planar truncation of the bulk structure, but that stepped regions exist on the surface. In the present work we perform calculations utilizing four and five phase shifts and investigate the effects of displacing the surface layer from the position it would

have if the bulk of the crystal were simply terminated.

In Figs. 5-8 we present a comparison between the experimental data of Jona²¹ for the aluminum (110) surface and calculations we have performed using various models of the surface-layer geometry. In these figures we present the results for the (00), (10), (01), and (11) beams, respectively. All curves are computed for a normally incident electron beam except for the dotted curve in Fig. 5(d), for which the beam enters the crystal at an angle $\theta = 5^\circ$ from the surface normal and an azimuthal angle $\phi = 90^\circ$.

In all the computed curves presented in this paper we have used the Lundqvist form for the complex electron self-energy $\Sigma(E) = \Sigma_1(E) - i\Sigma_2(E)$, and have shifted the final curves by an additional 3.65 eV to account for the work function of the

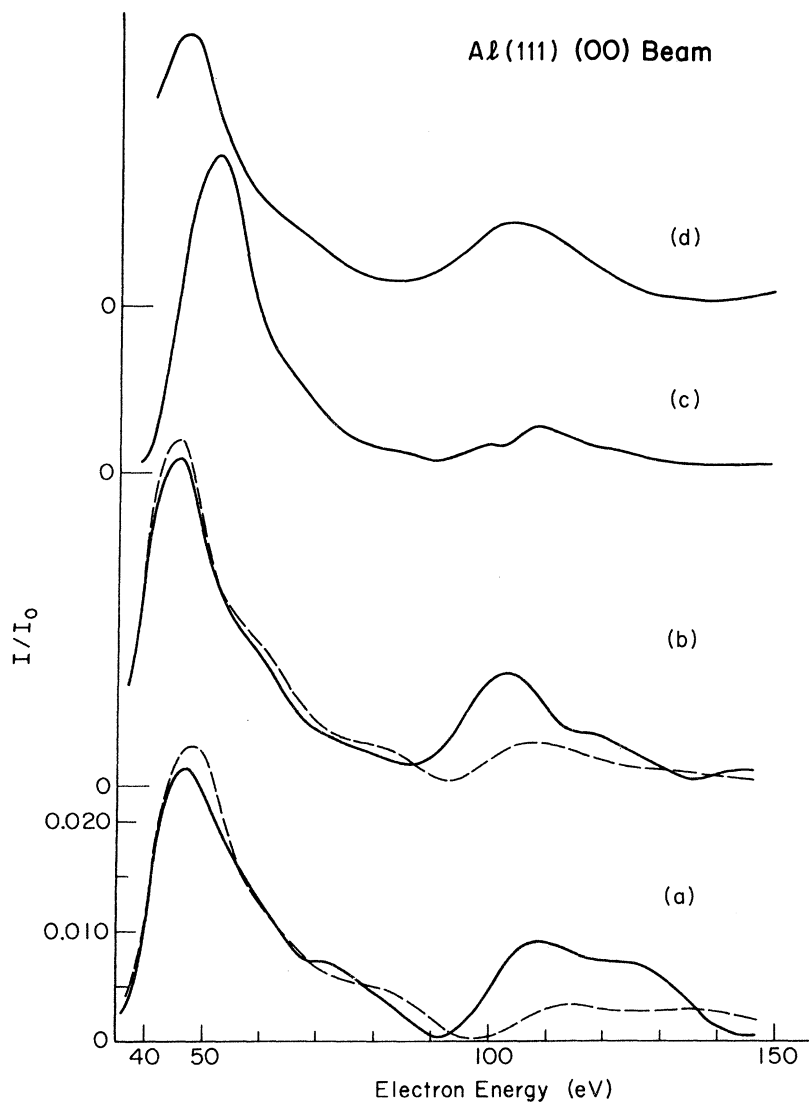


FIG. 9. Experimental I -vs- eV curve (c) compared to calculated curves for the (00) beam of the aluminum (111) surface. The solid curves [(a), (b), (d)] utilize five phase shifts and four layers in the computation. The dashed curves (a) and (b) utilize four phase shifts and three layers. Curve (a) is obtained from a surface whose outer-layer spacing is contracted by 5% of the bulk value to 2.216 Å. Curve (b) is obtained from an undistorted surface in which the outer-layer spacing is equal to that in the bulk, 2.33 Å. Curve (d) is computed for an electron beam incident at $\theta = 5^\circ$ and $\phi = 30^\circ$ with a surface layer spacing equal to that in the bulk. The experimental curve (c) is measured for incident beam angles $\theta = 5^\circ$ and $\phi = 30^\circ$. The theoretical curves are all shifted by 4.05 eV to account for the metallic work function.

metal.²⁴ The I -vs- eV curve [Fig. 5(a)] calculated for the (00) beam is seen to have its most prominent peak 13 eV lower in energy than the corresponding experimentally observed peak. Similarly, the smaller peak near 90 eV is 6 eV lower than experiment. Results obtained for the nonspecular beams (Figs. 6–8) show the same general characteristic whereby the calculated major and minor peak positions are about 5 eV lower in energy than the experimental values. It has been suggested that a contraction of the spacing between the surface layer and the bulk of the order of 10% might suffice to shift the calculated peak positions into agreement with experiment.¹⁷ In the curves labeled (b), (d), and (e) we perform contractions by 10, 15, and 20%, respectively, yielding surface layer to bulk spacings of 1.285, 1.214, and 1.142 Å. The expected energy shift of the peak positions occurs, as well as changes in the ratios of the peak intensities. Comparison of the calculated solid curves of Figs. 5(b) and 5(d) with the experimental curve [Fig. 5(c)] shows that the relative intensity ratios of the two prominent (00) beam peaks are in good agreement with experiment for an outer-layer contraction of 10–15% of the bulk interlayer spacing. Laramore and Duke¹⁷ have pointed out that the secondary structure obtained in their work near 100 eV in the (00) beam is too small with respect to their peak near 70 eV. The agreement we have achieved is improved partly due to the contraction we have introduced into the outer-layer spacing, and more significantly, as can be seen by reference to Fig. 2, by the inclusion of five phase shifts instead of three. Examination of curve (e) in Fig. 5 indicates that a con-

traction of 20%, leading to an outer-layer spacing of 1.142 Å, shifts the peak appearing near 70 eV to an energy 5 eV in excess of the experimental result. Furthermore, a lower-energy peak of about the same magnitude appears to be emerging near 40 eV in contradiction to the observed (00) beam curve (c).

The calculated results for the nonspecular beams (Figs. 6–8) are likewise seen to improve upon contraction of the outermost-layer spacing. The peaks in the 100–130-eV region for both the (01) and (10) beams are seen to shift to higher energies and to diminish in magnitude with respect to the peaks near 50 eV. The results for the (11) beam are included for completeness, but the absence of multiple prominent peaks makes peak-intensity comparisons impossible since only the relative intensities were measured experimentally. The over-all qualitative agreement between calculated and experimental nonspecular curves appears to occur at an outer-layer spacing near 10% and less than 15% contraction from the bulk interlayer distance.

The most serious discrepancies remaining unresolved in the present calculations occur in the 40–60-eV energy region for the nonspecular beams. In Fig. 6 a peak near 50 eV is visible for all the contractions for which we have performed calculations, but the peak never approaches the sharpness of the experimental peak, and this makes it difficult to obtain a meaningful intensity ratio between this peak and the one near 105 eV. In Fig. 7 for the (10) beam, the relative intensities of the two peaks near 45 and 65 eV are in good agreement for a layer contraction between 10 and

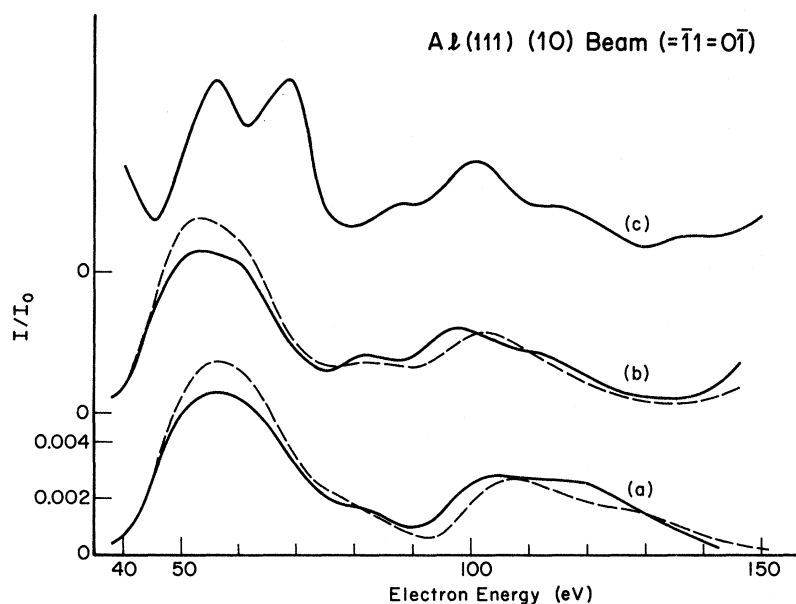


FIG. 10. Experimental I -vs- eV curve (c) is compared to calculated curves for the (10) beam [= $(\bar{1}1) = (0\bar{1})$] of the aluminum (111) surface. The description of curves (a) and (b) are given in the caption to Fig. 9. All curves are computed or measured at normal incidence.

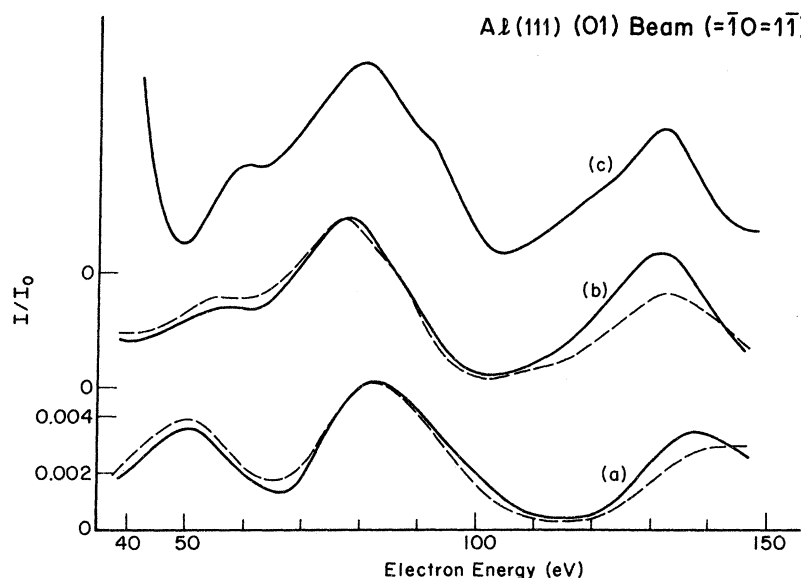


FIG. 11. Experimental I -vs- eV curve (c) is compared to calculated curves for the (01) beam [$(\bar{1}0) = (1\bar{1})$] of the aluminum (111) surface. The description of curves (a) and (b) are given in the caption to Fig. 9. All curves are computed or measured at normal incidence.

15%, but the small experimentally observable peak at 56 eV cannot be resolved in these calculations.

In conclusion, we believe that the comparison of all four diffracted beams of Figs. 5–8 is sufficient to establish that the spacing between the aluminum (110) surface layer and the bulk is contracted from the bulk interlayer spacing by an amount equal to 10–15% of that value, i. e., an interlayer spacing of 1.285–1.214 Å. This conclusion is based on the qualitative shapes of all four curves, peak positions, and relative peak intensities. We emphasize the point that for LEED calculations of presently attainable accuracy it is dangerous to rely exclusively on relative peak amplitudes or on peak positions which may be altered by several eV by small changes in the ion-core potential or by the model used to describe the complex electron self-energy $\Sigma(E)$.

V. ALUMINUM (111)

Calculated I -vs- eV curves are plotted in Figs. 9–11 for the (00), (10), and (01) beams of the aluminum (111) surface. Included in each plot for reference is the experimental curve from the work of Jona²¹ [Figs. 9(c), 10(c), and 11(c)]. Four calculations are made for each beam. Two of them treat the (111) surface as a simple truncation of the bulk structure and the other two are calculated by assuming a 5% contraction in the spacing between the outermost two layers. The dashed curves in each case represent calculations in which four phase shifts and three layers parallel to the surface are included. The solid curves include five phase shifts and four layers.

For all three beams considered, the calculation

using five phase shifts and an undistorted crystal surface yields results in closest agreement with the experimental curve. The calculated peak positions for the (00) beam are in close agreement with the experimental peaks without making a shift of 4.05 eV to account for the work function of the metal.²⁴ However, the relative magnitudes of the two peaks are quite different in each case. This is not unexpected since the calculations are performed at normal incidence and the experimental measurements for the (00) beam are taken at $\theta = 5^\circ$ and $\phi = 30^\circ$. The qualitative agreement between the calculation and experiment is improved by performing the computation for an incident beam impinging at these angles [Fig. 9(d)]. The two nonequivalent nonspecular beams show similar agreement between the positions of the experimental and theoretical maxima (Figs. 10 and 11). In these cases, moreover, the relative intensities of the various peaks are also in good agreement as are their qualitative shapes.

A rather small outer-layer distortion (contraction by 5% of the interlayer spacings from 2.33 to 2.216 Å) suffices to shift the calculated curves to higher energies, and to qualitatively alter the shapes and intensity ratios of the various peaks. We believe that the cumulative evidence from the three beams considered is sufficient to establish that the spacing between the outermost two layers of the aluminum (111) surface is identical to the bulk spacing to within less than 5%.

The good qualitative agreement attained in this case allows us to point out certain limitations in calculations of this degree of accuracy. The ion-core potential calculated by the method of Pendry¹⁶ is sufficient to give the agreement obtained here,

but does not allow the resolution of the 50–60-eV peak of the (01) beam into the double-peak structure seen in the experimental curve. A similar instance was noted in Sec. IV for the (10) beam of the aluminum (110) surface in the same energy region. Discrepancies in the low-energy ($\lesssim 50$ eV) peak positions for the (111) surface are of the same magnitude as those observed with the (110) surface and indicate that such effects are attributable to the form of the ion-core potential, or

to the model employed for the complex electron self-energy rather than to the geometrical arrangement of the crystal layers in the surface region.

ACKNOWLEDGMENTS

This work was supported by the U. S. Atomic Energy Commission. The authors are grateful to Dr. J. B. Pendry for supplying the computer program used to calculate the ion-core phase shifts.

¹J. B. Pendry, *J. Phys. C* **2**, 2273 (1969); *J. Phys. C* **2**, 2283 (1969).

²G. Capart, *Surf. Sci.* **26**, 429 (1971).

³J. A. Strozier, Jr. and R. O. Jones, *Phys. Rev. B* **3**, 3228 (1971).

⁴J. L. Beeby, *J. Phys. B* **1**, 82 (1968).

⁵C. B. Duke and C. W. Tucker, Jr., *Surf. Sci.* **15**, 231 (1969).

⁶C. B. Duke, J. R. Anderson, and C. W. Tucker, Jr., *Surf. Sci.* **19**, 117 (1970).

⁷D. W. Jepsen, P. M. Marcus, and F. Jona, *Phys. Rev. Lett.* **26**, 1365 (1971); *Phys. Rev. B* **5**, 3933 (1972).

⁸D. W. Jepsen and P. M. Marcus, *Computational Methods in Band Theory* (Plenum, New York, 1971), p. 416.

⁹S. Y. Tong and T. N. Rhodin, *Phys. Rev. Lett.* **28**, 553 (1972).

¹⁰R. H. Tait, S. Y. Tong, and T. N. Rhodin, *Phys. Rev. Lett.* **28**, 553 (1972).

¹¹J. B. Pendry, *Phys. Rev. Lett.* **27**, 856 (1971).

¹²G. E. Laramore and C. B. Duke, *Phys. Rev. B* **2**, 4782

(1970).

¹³C. W. Tucker, Jr. and C. B. Duke, *Surf. Sci.* **24**, 31 (1971).

¹⁴J. B. Pendry, *J. Phys. C* **4**, 3095 (1971).

¹⁵E. C. Snow, *Phys. Rev.* **158**, 683 (1967); *Phys. Rev.* **171**, 785 (1968).

¹⁶J. B. Pendry, *J. Phys. C* **4**, 2501 (1971).

¹⁷G. E. Laramore and C. B. Duke, *Phys. Rev. B* **5**, 267 (1972).

¹⁸G. E. Laramore, C. B. Duke, A. Bagchi, and A. B. Kunz, *Phys. Rev. B* **4**, 2058 (1971).

¹⁹J. B. Pendry (private communication).

²⁰P. M. Marcus, D. W. Jepsen, and F. Jona, *Surf. Sci.* **31**, 180 (1972).

²¹F. Jona, *IBM J. Res. Dev.* **14** (4), (1970).

²²B. I. Lundqvist, *Phys. Status Solidi* **32**, 273 (1969).

²³G. E. Laramore, J. E. Houston, and R. L. Park (to be published).

²⁴N. D. Lang and W. Kohn, *Phys. Rev. B* **3**, 1215 (1971).

Low-Energy-Electron-Diffraction Intensity Profiles and Electronic Energy Bands for Lithium Fluoride*

G. E. Laramore and A. C. Switendick

Sandia Laboratories, Albuquerque, New Mexico 87115

(Received 4 October 1972)

Model calculations of the low-energy-electron-diffraction (LEED) intensity profiles for LiF (100) and of the bulk electronic energy bands for LiF are performed using model potentials with quite different degrees of ionicity. One potential is constructed using Li^0 and F^0 free-atom charge densities and the other is constructed using Li^+ and F^- free-ion charge densities. Although both model potentials yield rather similar band gaps, the photoemission threshold and LEED measurements clearly favor the Li^+F^- form of the potential. Experimental LEED intensity profiles for LiF (100) at $T=573$ °K are analyzed, and certain features strongly suggest that the top lithium and fluorine sublayers do not lie in the same plane but are separated by about 0.25 Å in a direction normal to the surface. In order to motivate further experimental work, additional intensity profiles are calculated for both the perfect surface model and the reconstructed surface model.

I. INTRODUCTION

Thus far, all low-energy-electron-diffraction (LEED) calculations utilizing a microscopic model for the electron-ion-core potential have dealt with scattering from metal surfaces. In spite of the

complete neglect of the effects of surface morphology and the use of bulk electron-ion-core potentials, in many instances these calculations have achieved a reasonable correspondence with experimental measurements of LEED intensities.¹⁻⁹ However, the intrinsic interest in LEED as a tool